J. Fluid Mech. (2005), *vol.* 533, *pp.* 259–268. © 2005 Cambridge University Press
doi:10.1017/S0022112005004441 Printed in the United Kingdom

Turbulent entrainment into natural gravity-driven flows

By M. PRINCEVAC[1]†, H. J. S. FERNANDO[1] AND C. D. WHITEMAN[2]‡

[1]Environmental Fluid Dynamics Program, Department of Mechanical and Aerospace Engineering, Arizona State University, Tempe, AZ 85287-9809, USA

[2]Pacific Northwest National Laboratory, Richland, WA 99352, USA

(Received 31 October 2004 and in revised form 4 March 2005)

Observations of entrainment into natural gravity-driven flows on sloping surfaces are described. It is shown that the laboratory-based entrainment law of Ellison & Turner (1959), which is often used for modelling of atmospheric and oceanic flows, underestimates the entrainment rates substantially, arguably due to the fact that the laboratory flows have been conducted at Reynolds numbers ($Re \lesssim 10^3$) below what is required for mixing transition ($Re \sim 10^3$–10^4) whereas natural flows occur at much higher Reynolds numbers ($Re \sim 10^7$). A new entrainment law of the form $E \sim Ri^{-3/4}$ is proposed for the atmospheric Richardson number range $0.15 < Ri < 1.5$. In contrast to the laboratory observation that entrainment ceases at $Ri = 0.8$, field observations show continuous entrainment over the entire Richardson number range.

1. Introduction

The incorporation of ambient fluid into a flowing layer of turbulent fluid across the interface that separates them (i.e. the entrainment phenomenon) has long been a subject of investigations that date back to Rouse & Dodu (1955). Entrainment is widespread in engineering and environmental flows (List 1982; Turner 1986), some examples being the spreading of fire plumes, dilution of methane in coal mines and sewage in ocean outfalls and the growth of lower-atmospheric and upper-oceanic mixed layers (Fernando 1991). Different forms of entrainment have been identified, the most common being entrainment into a mean current of characteristic velocity U via a flow with velocity w_H normal to the interface as shown in figure 1 in the context of a gravity current flowing along a uniform surface with inclination angle α. This type of entrainment also occurs in free turbulent shear layers such as jets, plumes and wakes. The well-known Morton–Turner–Taylor entrainment hypothesis was developed for this case (Hunt, Rottman & Britter 1983; Turner 1986), namely

$$\frac{|w_H|}{U} = E, \tag{1.1}$$

where E is the entrainment coefficient. For homogeneous (non-density-stratified) environments, E is a constant that depends on the type of flow and the definition of U. Other forms of entrainment and entrainment velocities have been proposed (Hunt

† Present address: Department of Mechanical Engineering, University of California Riverside, CA 92521, USA.

‡ Present address: Department of Meteorology, University of Utah, UT 84112, USA.

https://doi.org/10.1017/S0022112005004441 Published online by Cambridge University Press

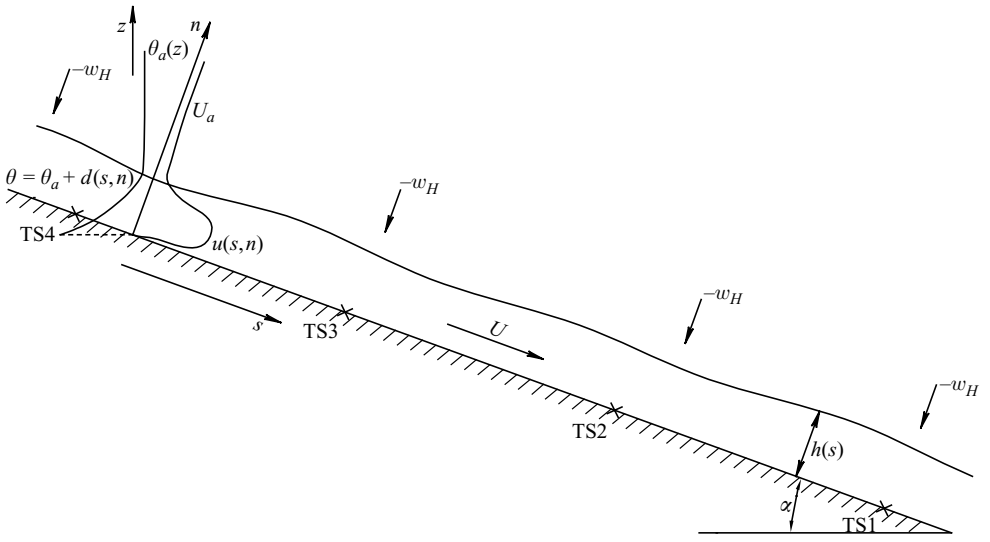


FIGURE 1. A schematic of a gravity current draining down a uniform slope. This figure is a definition diagram for subsequent discussions. In the field experiments to be discussed later, four tethered balloons TS1, TS2, TS3 and TS4 were deployed to obtain vertical profiles of velocity and temperature.

et al. 1983), including a boundary entrainment velocity w_B, defined as the rate at which the turbulent/non-turbulent boundary (i.e. the entrainment interface) spreads into the ambient flow, and the flux entrainment velocity w_F, a characteristic velocity with which scalar quantities cross the entrainment interface. If the thickness of the turbulent layer is h and the concentration difference across and the concentration flux through the interface are ΔC and $\overline{c'w'}$, respectively, then

$$|w_H| = \frac{\partial Uh}{\partial x}, \quad w_B = \frac{\mathrm{d}h}{\mathrm{d}t}, \quad w_F = \frac{\overline{c'w'}}{\Delta C}. \tag{1.2}$$

When buoyancy effects are present, the entrainment coefficient is no longer a constant, but is a function of (a suitably defined) Richardson number Ri. The form of $E(Ri)$, which is also known as the Entrainment Law, has been studied extensively using laboratory and numerical experiments (Fernando 1991). One of the earliest and often quoted laboratory experiments is that of Ellison & Turner (1959), wherein entrainment into a gravity current originating from an upstream negatively buoyant fluid source was studied (see figure 1), and an entrainment law of the form (Turner 1986)

$$E = \frac{0.08 - 0.1Ri}{1 + 5Ri} \quad \text{for} \quad Ri \leqslant 0.8, \tag{1.3}$$

was identified. Here $Ri = \Delta bh\cos\alpha/U^2$, where $\Delta b = g\Delta\theta/\theta_R$ is a characteristic buoyancy jump across the entrainment interface corresponding to the temperature jump $\Delta\theta = \theta(n=h) - \Theta$ between the layer-averaged temperature Θ and the temperature at the top of the interface, g the gravitational acceleration, n the normal coordinate to the slope, and θ_R a reference temperature (see § 2 for the general form of Ri). Ellison & Turner's experiments were conducted over a range of slopes $10^\circ < \alpha < 90^\circ$ with a uniform ambient temperature θ_a, so that the ambient temperature gradient $\partial\theta_a/\partial z = 0$, where z is the vertical coordinate. The entrainment was found to cease for $Ri \geqslant 0.8$.

https://doi.org/10.1017/S0022112005004441 Published online by Cambridge University Press

In a few instances entrainment measurements in oceans and the atmosphere are available but they are very limited in extent and do not address the dependence of E on Ri. In a case relevant to this paper, Horst & Doran (1986) inferred entrainment into nocturnal downslope (katabatic) winds along a 21° slope on Rattlesnake Mountain near Richland, WA. They used three towers and one tethered balloon, and compared the height h measurements of katabatic winds with those inferred by the formula proposed by Manins & Sawford (1979)

$$h = 0.75Es, \tag{1.4}$$

and the empirical fit to Ellison & Turner's (1959) data by Briggs (1981),

$$E \approx 0.05 \sin\alpha^{2/3}, \tag{1.5}$$

where s is the along-slope coordinate.

A broad agreement between the measurements and predictions of h was found, but only a few observational cases were considered and the Ri dependence of E was not studied. Note that as pointed out by Briggs (1981), (1.5) applies only to slope angles greater than 12°, and hence may not be applicable for the low slope angles considered in this paper.

Ellison & Turner's entrainment law (1.3) has been extensively utilized in modelling of atmospheric (Manins & Sawford 1979; Nappo & Rao 1987) and oceanic (Baines 2002) flows. Questions linger, however, with regard to its applicability to high-Reynolds-number (Re) natural flows, such as atmospheric nocturnal downslope (katabatic) flows that have typical Reynolds numbers on the order $Re \approx Uh/\nu \sim 10^7$, where ν is the kinematic viscosity. Citing Batchelor & Townsend's (1956) review that suggested possible molecular effects even at high Re, Ellison & Turner themselves cautioned on the use of their results (obtained with $Re \leqslant 10^3$) in natural flow situations. Briggs (1981) also arrived at the same conclusion. This claim of Re effects has been further buttressed by the discovery of the 'mixing transition' phenomenon, which suggests that a minimum critical Reynolds number Re_{cr} must be exceeded to sustain three-dimensional inertially dominated turbulent fluctuations in a shear flow. Accordingly, a sharp increase of mixing activity occurs above Re_{cr}, leading to enhanced mixing rates that are independent of Re (Konrad 1976). Dimotakis (2000) estimated an empirical Reynolds number of $Re_{cr} \approx 10^4$, but the value suggested by Breidenthal (1992) is $Re_{cr} \approx 10^3$. The Prandtl (or Schmidt) number may also play a role, at least at low Re, as pointed out by Breidenthal (1992), Yeung, Shuyi & Sreenivasan (2002), and Noh & Fernando (1993).

To verify the applicability of laboratory-based entrainment laws to natural very high-Reynolds-number situations, we have conducted entrainment observations in katabatic flows. These measurements were made in October 2000 during the Vertical Transport and Mixing Experiment (VTMX) sponsored by the Environmental Meteorology Program of the Department of Energy. The slope selected was gentle and uniform and was as close to an 'ideal' slope as could be achieved in the field. The measurements were conducted under weak synoptic flow conditions (Doran, Fast & Horel 2002), so that there was little influence from pressure-gradient-driven upper-level flows. During the periods selected for analysis, the cross-flows on the slopes were also small, less than 0.25 m s^{-1} vis-à-vis the 3–5 m s^{-1} along-slope katabatic winds. The theoretical basis of the flow analysis is described next, followed by the experimental procedure in § 3 and experimental results in § 4. The paper concludes with a discussion in § 5.

https://doi.org/10.1017/S0022112005004441 Published online by Cambridge University Press

2. Theoretical preliminaries

Consider, for simplicity, a two-dimensional gravity current flowing down a simple incline of angle α. The along-slope and normal-to-the-slope coordinates are s and n, respectively, and the corresponding vertical and horizontal coordinates are (x, y). For generality, assume the presence of a uniform background flow U_a relative to which the buoyancy-driven current has a velocity $u(s, n)$. Thus, the katabatic layer has a velocity $U_a + u(s, n)$. The usual layer-averaged quantities can then be defined as (Fleagle 1950; Ellison & Turner 1959)

$$\left.\begin{aligned} Uh &= \int_0^H u\,\mathrm{d}n, \quad U^2h = \int_0^H u^2\,\mathrm{d}n, \quad (U+U_a)Bh = \int_0^H (u+U_a)g'\,\mathrm{d}n, \\ S_1Bh^2 &= 2\int_0^H g'n\,\mathrm{d}n, \quad S_2Bh = \int_0^H g'\,\mathrm{d}n, \end{aligned}\right\} \tag{2.1}$$

where H is a suitable averaging height beyond which the perturbations due to buoyancy-driven u can be neglected, h, U and B are the characteristic thickness, velocity and buoyancy of the katabatic layer, respectively, $g' = gd/\theta_R$ is the reduced gravity, d is the deviation of temperature θ of the katabatic flow from the undisturbed ambient temperature $\theta_a(z)$ so that $\theta = \theta_a + d$ and S_1 and S_2 are shape factors. The integration of the continuity equation in the n-direction yields

$$\frac{\partial}{\partial s}\int_0^H (u+U_a)\,\mathrm{d}n + w_H = 0, \tag{2.2}$$

or

$$\frac{\partial}{\partial s}(Uh) = EU, \tag{2.3}$$

where w_H is the entrainment velocity, which can be expressed in terms of the entrainment coefficient as $w_H = -EU$. The integral form of the momentum equation, therefore, becomes

$$\frac{\partial}{\partial t}Uh + EU(U+U_a) + hU\frac{\partial U}{\partial s} = S_2Bh\sin\alpha - \frac{1}{2}\cos\alpha\frac{\partial}{\partial s}(S_1Bh^2) - C_D(U+U_a)^2, \tag{2.4}$$

where (2.3) has been used together with the parameterization for the surface drag $-C_D(U + U_a)^2$ based on the drag coefficient $C_D = [u_*/(U + U_a)]^2$, where u_* is the friction velocity (Manins & Sawford 1979). Note that, as pointed out by Manins & Sawford (1979), there are two important drag forces for katabatic flows: the surface drag and the 'interfacial drag' due to entrainment of ambient fluid into the katabatic flow. The ratio of these two effects becomes, from (2.4),

$$R_s = \frac{C_D(U+U_a)^2}{EU(U+U_a)} = \frac{C_D}{E}\left(1 + \frac{U_a}{U}\right). \tag{2.5}$$

The ratio R_s is important in modelling, as it gives guidance on what simplifications are plausible. For example, Manins & Sawford quoted a maximum C_D of 3×10^{-4}, and assumed that the surface stress term can be neglected. In the present work, we will evaluate both E and C_D and investigate how R_s changes with the Richardson number $Ri = Bh\cos\alpha/U^2$, which is the general form of Richardson number used by Ellison & Turner (1959).

https://doi.org/10.1017/S0022112005004441 Published online by Cambridge University Press



FIGURE 2. The Slope Site in the southwestern part of the Salt Lake Valley. The circles at the Slope Site mark the locations of tethersonde TS1 (right) and TS4 (left). KC is the Kennecott Copper mine.

3. Experimental setup

The principal goal of the VTMX campaign was to study transport and mixing processes in complex topography under (nocturnal) stable conditions. The details of the field campaign have been given by Doran *et al.* (2002). Nine national laboratories and three universities participated in the experiments, including the authors. The principal measurement site was called the Slope Site, and was located in the southwestern part of the Salt Lake Valley, east of the big Kennecott open pit copper mine KC (figure 2). This site is characterized by a gentle ($\alpha = 1.58^\circ$) and very smooth (aerodynamic roughness length ~ 0.1 m) slope extending over a 15 km distance. There were no man-made objects in the vicinity. The major topographic perturbation upstream of the site is the Oquirrh Mountain range abutting the gentle slope 10 km west of the measurement location. The site was equiped with a variety of instruments including a lidar, sodar, tethersondes and a sonic anemometer. For the present analysis only the tethersonde data consisting of velocity, pressure, height and humidity, transmitted to a ground station via a frequency synthesized transmitter, were used. The data from other instruments were used for checking the results, but data from these instruments were plagued by gaps. Four tethered balloons aligned along the west–east direction (40°32′21″ N), sited approximately 1 km apart, provided simultaneous vertical soundings of temperatures and winds. The tethersondes were named TS1 (112°01′30″ W), TS2 (112°02′12″ W), TS3 (112°02′54″ W), and TS4 (112°03′36″ W) (see figures 1 and 2).

https://doi.org/10.1017/S0022112005004441 Published online by Cambridge University Press

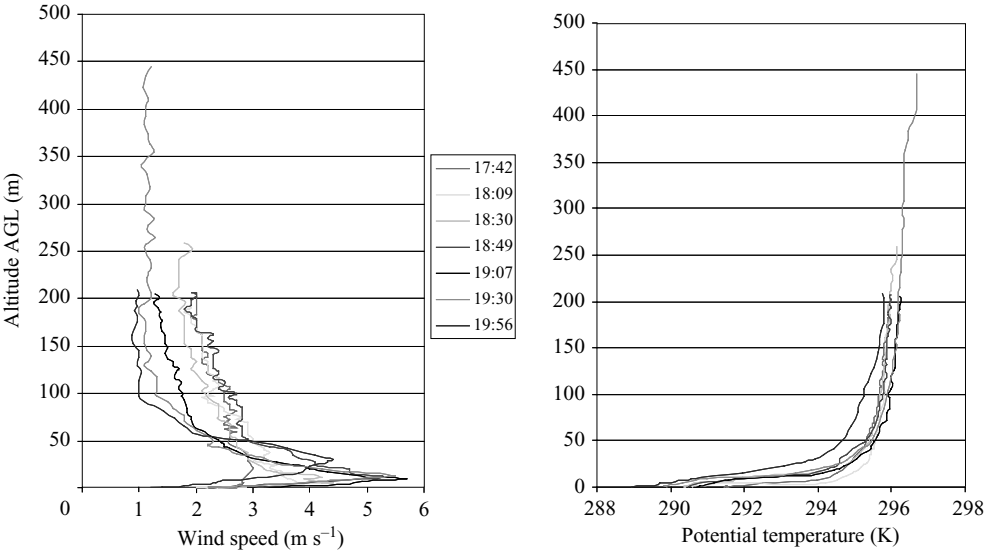


FIGURE 3. Representative tethersonde profiles of wind speed and potential temperature at the site (TS1). Numbers in the legend are Local Standard Time.

4. Experimental results

Three Intensive Observational Periods (IOPs) of the VTMX campaign have been identified as completely dominated by katabatic winds without significant synoptic influence (Doran *et al.* 2002) and these periods (October 14–15 IOP 5, 16–17 IOP 6 and 19–20 IOP 8) were used for analysis. Figure 3 shows the evolution of wind speed and potential temperature profiles throughout the early evening of October 14. Note the presence of well-defined katabatic winds (3–5 m s^{-1}) and a weak flow aloft (∼1–2 m s^{-1}) with $\partial U_a/\partial n$ small compared to the variation of winds within the downslope flow. Typical velocity profiles extended up to 200 m, with a few extending beyond. The contorted nature of the profiles above the katabatic layer can be construed as a result of the intrusions (detrainment flow) emanating from the katabatic layer, as observed in the laboratory experiments of Baines (2002). Although the velocity and temperature profiles slowly evolve in time (with maximum rates 2 m s^{-1} h^{-1} and 1–2 K h^{-1}), such changes occur at a much slower rate than processes associated with entrainment (having a time scale $h/U \approx 25$ s) and hence, for the purpose of entrainment calculations, the profiles were assumed quasi-stationary.

The data were quality assured, U, h, and B were calculated for selected profiles, and the entrainment velocity was evaluated using (2.3) with $\Delta s = 1$ km. The entrainment results are shown in figure 4, with error bars presenting the 90 % confidence intervals. The best fit curve is given by

$$E \approx 0.05 Ri^{-0.75} \tag{4.1}$$

for $0.15 < Ri < 1.5$. Note that, as $Ri \to 0$, this entrainment law is expected to take a different form and should approach that of non-stratified flows, and at large Ri it asymptotes to that of molecular diffusive mixing. Note that for $Ri < 0.8$ or so, the entrainment is significant ($E > 0.05$) and thus interfacial drag is expected to prevail. For $Ri > 0.8$, the entrainment rate becomes smaller, and the frictional resistance at the ground is expected to be of importance (see below). Perhaps, the entrainment mechanism changes at this critical Ri, for example, from powerful Kelvin–Helmholtz

https://doi.org/10.1017/S0022112005004441 Published online by Cambridge University Press

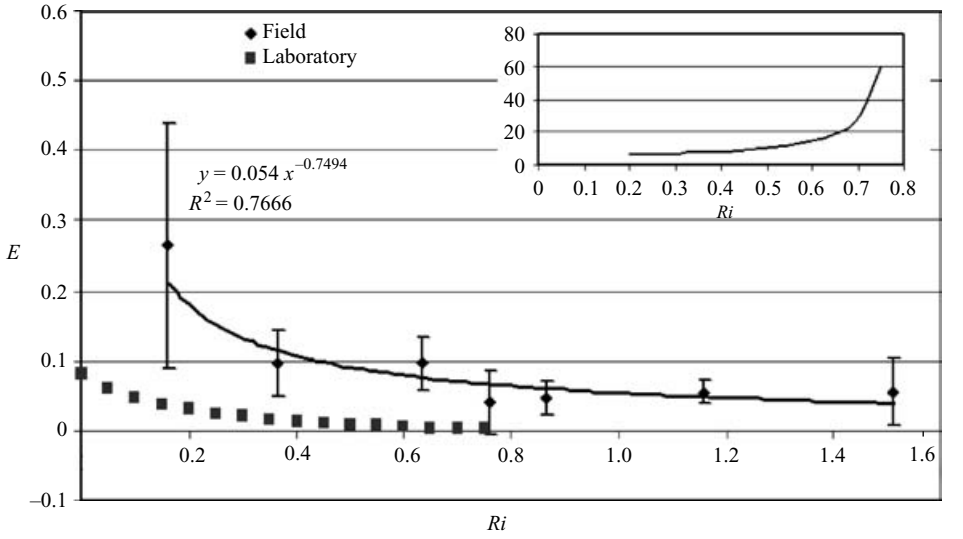


FIGURE 4. The entrainment coefficient evaluated using the field data. The error bars show 90 % confidence intervals. The laboratory data of Ellison & Turner (1959) are also shown. The ratio of the two lines is given in the inset.

(KH) instability-induced mixing to mixing caused by intermittent internal wave breaking and/or Hölmböe instability as found in the laboratory studies of Strang & Fernando (2001*a*, *b*). The wave breaking and/or Hölmböe regime has strikingly smaller entrainment rates due to the enhanced buoyancy influence. According to Strang & Fernando (2001*a*, *b*), the critical Richardson number for the transition between KH billowing and wave-breaking mixing regimes is approximately unity.

Several interesting features are evident from the measurements. First, the normalized entrainment rate $E = |w_H|/U$ on the slope is significantly larger than that of laboratory measurements: about a factor of five at $Ri \approx 0.2$ and an order of magnitude at $Ri \approx 0.5$. Second, in contrast to the laboratory observation that entrainment ceases at $Ri > 0.8$, the field measurements continue to show entrainment for Ri values as high as 1.5. These observations can be attributed to the low Reynolds numbers used for laboratory flows ($Re \leqslant 10^3$) as compared to those of natural flows ($Re \approx (3\text{–}5) \times 10^7$). The field Re are well above the mixing transition, and hence can sustain well-defined three-dimensional fluctuations that support enhanced mixing. Laboratory observations (Konrad 1976) conducted over a range of Re show a several-fold increase of the mixing rate at the mixing transition Reynolds number Re_{cr}, which is consistent with the high mixing rates of natural flows evident from figure 4. Finally, for the slope angle (1.58°) considered, Briggs' formula (1.5) gives an entrainment coefficient of $E \approx 5 \times 10^{-3}$, irrespective of Ri, which is not borne out by the measurements. This is consistent with the assertion that (1.5) may not be applicable for low slope angles.

The ratio of the entrainment coefficient to the surface drag coefficient is presented in figure 5, following (2.5). Note that the interfacial drag exceeds frictional drag for smaller Ri, but they become comparable at larger Ri. For this analysis, data from another VTMX site (Arizona Cemetery Site, ACS) operated by our group were used (Monti *et al.* 2002), since at ACS the sonic anemometer measurements of the surface-layer Reynolds stresses were made at the same location as the balloon measurements (whereas at the slope site they were separated by ~ 1 km). The drag coefficient was

https://doi.org/10.1017/S0022112005004441 Published online by Cambridge University Press

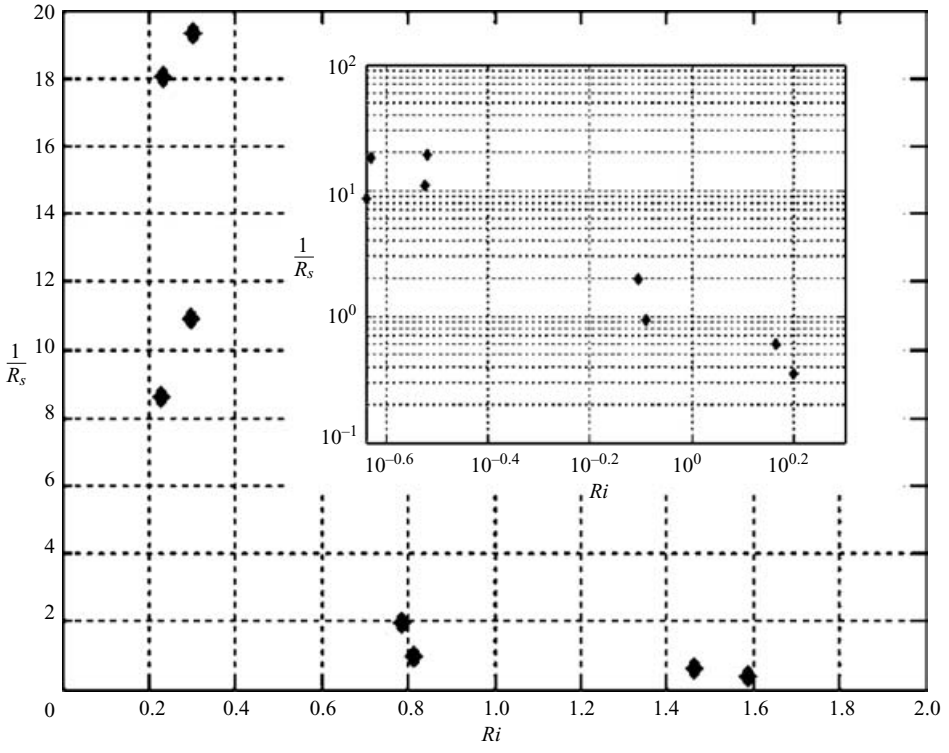


FIGURE 5. The ratio of the drag due to interfacial mixing and surface friction as a function of the Richardson number. For the convenience and clarity the log-log plot is also given in the inset.

calculated by using the expression $C_D = [u_*/(U + U_a)]^2$, and u_* was evaluated using Reynolds stress measurements. The ACS site provided only a limited number of data points, as evident from figure 5.

5. Conclusions

Field observations described herein indicate that the laboratory-based entrainment law of Ellison & Turner (1959), which is often used for modelling natural gravity-driven flows on slopes, substantially underestimates the entrainment coefficient of high-Reynolds-number natural flows. In addition, contrary to the laboratory findings, entrainment persists beyond $Ri \approx 0.8$, which has been identified, based on laboratory results, as the critical Richardson number Ri_{cr} above which the entrainment ceases. Both of these observations can be explained by considering the role of molecular diffusive effects in turbulent entrainment. First, laboratory flows have Reynolds numbers ($Re \leqslant 10^3$) lower than the critical Reynolds number Re_{cr} necessary to sustain fully inertial, three-dimensional turbulent fluctuations ($Re_{cr} \sim 10^3$–10^4) whereas natural flows have Reynolds numbers ($Re \sim 10^7$) much greater than Re_{cr}. Thus, the entrainment coefficient in Ellison & Turner's (1959) laboratory flow is expected to be lower. Second, as pointed out by Noh & Fernando (1993), the critical Richardson number Ri_{cr} for the suppression of turbulent entrainment in stratified flows is dependent on the Péclet number (Pe) of the flow, according to $Ri_{cr} \sim Pe^{1/2}$. Thus, the atmospheric critical Richardson number, equivalent to the laboratory-based

https://doi.org/10.1017/S0022112005004441 Published online by Cambridge University Press

Ellison & Turner's value of $Ri_{cr} = 0.8$ in water is about 25, which is rarely achieved in the atmosphere (this calculation assumes that the Ri_{cr}–Pe relationship is not significantly affected by the mixing transition).

The results also show that the entrainment drag dominates surface drag at $Ri < 0.8$ whereas it is of the same order as the surface friction drag for $Ri > 0.8$, indicating a notable change of entrainment mechanism at $Ri \sim 0.8$. This is consistent with the findings of Strang & Fernando (2001*a*, *b*) that entrainment mechanisms show distinct transitions at various Richardson number thresholds. Accordingly, at smaller Ri (< 1) the entrainment is governed by frequent Kelvin–Helmholtz instability events whereas at large Ri the entrainment is dominated by intermittent entrainment events due to breaking of interfacial waves or Hölmböe instabilities.

This research was mainly supported by the National Science Foundation (CTS/ATM) and the US Department of Energy (DOE) under the auspices of the Atmospheric Sciences Program of the Office of Biological and Environmental Research. C. D. W.'s contributions were made at DOE's Pacific Northwest National Laboratory, which is operated by Battelle. We wish to thank Drs Peter Baines and Christopher Doran for their useful comments.

REFERENCES

Baines, P. G. 2002 Two-dimensional plumes in stratified environments. *J. Fluid Mech.* **471**, 315–337.

Batchelor, G. K. & Townsend, A. A. 1956 Turbulent diffusion. In *Surveys in Mechanics*, pp. 352–399. Cambridge University Press.

Breidenthal, R. E. 1992 Entrainment at thin stratified interfaces: the effects of schmidt, Richardson and Reynolds numbers. *Phys. Fluids* A **4**, 2141–2144.

Briggs, G. A. 1981 Canopy effects on predicted drainage flow characteristics and comparison with observations. In *Proc. Fifth AMS Symposium on Turbulence and Diffusion, Atlanta, GA*. American Meteorological Society, Boston, MA.

Dimotakis, P. E. 2000 The mixing transition in turbulent flows. *J. Fluid Mech.* **409**, 69–98.

Doran, J. C., Fast, J. D. & Horel, J. 2002 The VTMX 2000 campaign. *Bull. Am. Met. Soc.* **83**, 537–551.

Ellison, T. H. & Turner, J. S. 1959 Turbulent entrainment in stratified flows. *J. Fluid Mech.* **6**, 423–448.

Fernando, H. J. S. 1991 Turbulent mixing in stratified fluids. *Annu. Rev. Fluid Mech.* **23**, 455–493.

Fleagle, R. G. 1950 A theory of air drainage. *J. Met.* **7**, 227–232.

Horst, T. W. & Doran, J. C. 1986 Nocturnal drainage flow on simple slopes. *Boundary-Layer Met.* **34**, 263–286.

Hunt, J. C. R., Rottman, J. W. & Britter, R. E. 1983 Some physical processes involved in the dispersion of dense gases. In *Proc. IUTAM Symp. On Atmospheric Dispersion of Heavy Gases and Small Particles*, Delft (ed. G. Oomes & H. Tennekes), pp. 361–395. Springer.

Konrad, J. H. 1976 An experimental investigation of mixing in two dimensonal turbulent shear flows with applications to diffusion limited chemical reactions. PhD thesis, California Institute of Technology. Project SQUID Report CIT-8PV.

List, E. J. 1982 Turbulent jets and plumes. *Annu. Rev. Fluid Mech.* **14**, 189–212.

Manins, P. C. & Sawford, B. L. 1979 A model of katabatic winds. *J. Atmos. Sci.* **36**, 619–630.

Monti, P., Fernando, H. J. S., Princevac, M., Chan, W.-C., Kowalewski, T. A. & Pardyjak, E. R. 2002 Observations of flow and turbulence in the nocturnal boundary layer over a slope. *J. Atmos. Sci.* **59**, 2513–2534.

Nappo, C. J. & Rao, K. S. 1987 A model study of pure katabatic flows. *Tellus* **39**A, 61–71.

Noh, Y. & Fernando, H. J. S. 1993 The role of molecular diffusion in the deepening of the mixed layer. *Dyn. Atmos. Oceans.* **17**, 187–215.

Rouse, H. & Dodu, J. 1955 Turbulent diffusion across a density discontinuity. *Houille Blanche* **10**, 522–532.

https://doi.org/10.1017/S0022112005004441 Published online by Cambridge University Press

Strang, E. J. & Fernando, H. J. S. 2001*a* Entrainment and mixing in stratified shear flows. *J. Fluid Mech.* **428**, 349–386.

Strang, E. J. & Fernando, H. J. S. 2001*b* Vertical mixing and transports through a stratified shear layer. *J. Phys. Oceanogr.* **31**, 2026–2048.

Turner, J. S. 1986 Turbulent entrainment: the development of the entrainment assumption, and its application to geophysical flows. *J. Fluid Mech.* **173**, 431–471.

Yeung, P. K., Shuyi, X. & Sreenivasan, K. R. 2002 Schmidt number effects on turbulent transport with uniform mean scalar gradient. *Phys. Fluid* **14**, 4178–4191.

https://doi.org/10.1017/S0022112005004441 Published online by Cambridge University Press